# THE EFFECT OF MASS FLOW RATE OF WHEAT SOLID PARTICLES ON CHARACTERISTICS OF ACOUSTIC SIGNALS IN PNEUMATIC CONVEYING
/
# اثر دبی جرمی ذرات جامد گندم در انتقال نیوماتیکی بر ویژگی‌های سیگنال‌های صوتی

**Ph.D. Stud. Mehdi Samadi[1], As Prof. Vahid Rostampour*[1], Prof. Shamsoallah Abdollahpour[2]**
[1] Urmia University, Department of Mechanical Engineering, Iran
[2] Tabriz University, Department of Mechanical Engineering, Iran
*Tel: 00984432779558; E-mail: v.rostampour@urmia.ac.ir*

***Keywords:*** *Acoustic, Mass Flow Rate, Pneumatic Convey, Wheat*

## ABSTRACT

*In the industry, the pneumatic conveying of wheat grains has attracted a lot of attention due to benefits such as enclosed transfer and flexibility in routing. Measuring the mass flow of wheat grains is important to avoid problems such as wear of the transmission pipes, pipeline clog due to dense phase and fracture of the seeds. In this research, the acoustic signal analysis method was used to detect the mass flow rate of wheat grains at three levels of 1.5, 3 and 4.5 kg/min in the pneumatic conveying. The signals decomposition was done in time-frequency domain (wavelet transform) with 9 levels. The properties of Sum, Mean, Variance (VAR), Root Mean Square (RMS), Skewness, Kurtosis, and Moment were compared. The results showed that the first ($d_1$), second ($d_2$), fifth ($d_5$), sixth ($d_6$) and seventh ($d_7$)* detail *sub-signals have the highest ability and priority to detect mass flow levels, respectively. Also among the studied properties, sum, mean, VAR, RMS, and moment, are prioritized for detecting mass flow levels with probability level of 1%, respectively. The values of all these properties increased with increasing mass flow rate. The acoustic signal analysis technique has a good potential for detecting the different mass flow levels of conveyed wheat grains.*

## چکیده

*انتقال نیوماتیکی دانه‌های گندم به دلیل مزایایی از قبیل انتقال به شکل محصور و قابلیت انعطاف‌پذیری در مسیریابی در صنعت مورد توجه زیادی قرار گرفته است. اندازه گیری دبی جرمی دانه های گندم به منظور جلوگیری از بروز مشکلاتی مانند سایش لوله های انتقال، گرفتگی لوله در اثر فاز غلیظ و شکستگی دانه‌ها حائز اهمیت میباشد. در این تحقیق، برای تشخیص میزان دبی جرمی عبوری دانه های گندم در سه سطح 1/5، 3 و 4/5 کیلوگرم در دقیقه از روش آنالیز سیگنالهای صوتی در حوزه زمان-فرکانس (تبدیل ویولت) استفاده گردید. تجزیه سیگنالها در 9 سطح انجام شد و ویژگیهای Sum، Mean، VAR، RMS، Skewness، Kurtosis، و Moment مورد مقایسه قرار گرفتند. نتایج نشان داد که زیرسیگنالهای دیتلز اول، دوم، پنجم، ششم و هفتم به ترتیب دارای بیشترین توانایی و اولویت برای تشخیص سطوح مختلف دبی های جرمی از یکدیگر می باشند. در بین ویژگی های بررسی شده به ترتیب ویژگی های Sum، Mean، VAR، RMS و Moment برای تشخیص دبی های جرمی با سطح احتمال 1% دارای اولویت هستند. مقادیر همه این ویژگی ها با افزایش دبی جرمی افزایش یافت. تکنیک صوت دارای پتانسیل خوبی جهت تشخیص سطوح مختلف دبی جرمی دانه های گندم در حال انتقال بود.*

## INTRODUCTION

The pneumatic conveying encompasses transmission of wide range of powdered and granular solids in gas stream (*Klinzing et al., 2009*). Pneumatic conveying has been popular in the industry for many decades because of advantages such as enclosed conveying of products and its flexibility in routing (*Mills, 2013*). Some of the industries that convey materials in pneumatic way include agriculture, chemistry, pharmaceuticals, mine, food, steel, plastic and rubber. Today, this method is used in flour mills to transport wheat from trailers and trucks to storage silos and vice versa, as well as the transfer of raw material from silos toward the flour milling process. The transfer of materials to the wheat silos due to its high height and volume is complicated and various methods are used for this purpose. The pneumatic conveying due to its high speed of material transfer in proportion to its volume, low cost of service and maintenance, least number of needed users and the controllability of the system in different working conditions, has been welcomed.

The mass flow control of solid particles in the pneumatic conveying system is very important *(Zheng and Liu, 2011*) .One of the visible problems in transfer of wheat grains is the wear of the transfer pipes, which is caused by frequent contact with the pipe walls. The other problem is the fracture of the seeds during the transfer, which is very important because it reduces the seed vigor and causes a disorder in the quality of the produced flour. One of the causes of seed fractures is the non-controlling material flow rate inside the pipe and the contact of the wheat grains with each other, as well as in the walls, especially in the knees. Also, the maximum utilization of energy in the pneumatic conveying system has barriers such as pipe clogging due to massive material mass concentration in the bottom of the pipes which, if not eliminated, will result in considerable energy losses and consequently increase the increased costs.

Different methods are used to measure the mass flow rate of solids in gas-solid medium in pneumatic transmission. Capacitive sensor is used to measure the mass flow rate of solid particles. These sensors has not been welcomed because of its sensitivity to moisture, size and heterogeneity and the chemical composition of solid particles (*Yan, 1996*). In radiometric measurement systems, ionization radiation is used in the form of gamma and x-rays to measure the mass flow rate of solids *(Van et al., 1993*). This system is not suitable for online measurement due to its high cost and safety constraints. One of the most widely used sensors is the optical sensor. In these sensors, the intensity of light passing through the diluted solid gas mixture depends on the volume concentration of solid matter. The major problem of optical sensors is the presence of a contaminated window and its asymmetry when entering and leaving, which can respond false signals and data. Tomography methods are powerful tools for measuring the volume concentration of solid particles moving in pneumatic transition pipe. Among the tomographic measurement systems, two methods of electrical capacity tomography (ECT) and electrical optical tomography (EOT) are used due to their high development. In general, in tomography, the definition level is poor and the sensitivity is very low. Also, using this method, strong dust is generated inside the pipe. The use of digital imaging because of the limited programming capability for dense and concentrated environments cannot be a suitable method for measuring mass flow rate. The flow meter based on the coriolis force (coriolis meter) has measurement limitations due to its difficult installation and the development of strong dust in the tube. Thermal gas flow meters are faced with reduced accuracy with the presence of different compositions of gas and show weak repeatability. Electrostatic sensors are sensitive to moisture, particle size, chemical composition and heterogeneity of particles, and also have high error levels of about 15%. Zheng and Lee provided a review of these methods (*Zheng and Liu, 2011*). Among the available techniques, the acoustic analysis method is attractive because of its advantages such as the relevance of the optimum frequency with particle size, the simplicity of the method, the robustness against difficult conditions, easy installation, online display, equipment costs and low maintenance (*Fuchs et al., 2008*). In this method, a microphone is used to record the sound produced by the materials flow (*Dhoriyani et al., 2006*). Based on the analysis of the density of the power spectrum and wave transfer, a theory on the relationship between the propagation of sound propagation and the mass flow rate of solid particles in the pneumatic convey could be established (*He et al., 2014*). The effect of the locating and positioning of acoustic sensors in the transmission pipe and the verification of their measurement in developing regions, especially after the 90 degree bends, has been investigated (*Tallon et al., 2000*). A new measurement system was developed for the detection of wood components in pneumatic conveying using vibration and sound sensors (*Sun et al., 2014*). Their results showed that both vibration and sound sensors can be used to detect the collisions between particles and the pipe wall. Also, the sound signal, if used with obstruction, has a higher SNR (Signal to-Noise Ratio) than the vibration signal, which is an advantage. A new method based on the passive sound propagation technique was established for the analysis of the particle-wall collision and friction (*He et al., 2014*). Wavelet conversion was used to extract information from particles and walls, as well as friction. According to these analyzes, a theoretical relationship was developed to establish a relationship between the AE (Acoustic Emission) signals and the ratio of solid loading in the vertical pneumatic convey pipe. The error obtained for the mass flow rate of solids using this model was less than 6.62%.

In the present study, a microphone with a high frequency range was used to record audio signals from wheat grains in the transfer pipes. The comparison of the signals in the time-frequency domain was performed and the Sum, Mean, Variance (VAR), Root Mean Square (RMS), Skewness, Kurtosis and Moment properties were used to detect different mass flow levels.

## MATERIALS AND METHODS

The research process, used equipment and a detailed description of acoustic signals processing are presented.

- **Research process and preparation of samples**

The acoustic signal analysis method was used to detect the mass flow rate of wheat grains at three levels of 1.5, 3 and 4.5 kg/min in the pneumatic conveying. The Bahar wheat cultivar as one of the most popular cultivars in Iran was used in the research. Wheat samples were prepared and transferred to the post-harvest laboratory to determine the physical and aerodynamic properties. Table 1 shows the physical and mechanical properties of the sample used.

**Table1**

**The physical and mechanical properties of the wheat**

| Physical and mechanical properties | Size |
|---|---|
| True density [kg/m$^3$] | 1325 |
| Bulk density [kg/m$^3$] | 815 |
| Sphericity coefficient [%] | 55.06 |
| Geometric grain diameter [m] | $4.35\times10^{-3}$ |
| Limit speed [m/s] | 12.41 |
| Saltation velocity [m/s] | 11.71 |
| Air required speed to prevent sedimentation [m/s] | 17.56 |

- **Equipment**

To pneumatic conveying the wheat grains in a solid-gas two-phase environment, a semi-industrial conveying system with a capacity of 1 ton/h was designed and constructed (Figure 1). In this system, a 0.5-hp centrifugal fan with working speed of 42 m/s, volumetric rate of 2.75 m$^3$/h and outlet diameter of 4.8 cm was used to supply the air needed for the convey. The feeder has 8 blades and the working capacity of 1 ton/h. The diameter of the transfer pipe is 4.8 cm and the length is 1.30 cm. The cyclone is centrifugal type with a cross sectional area of 78.5 cm$^2$.

In order to record the acoustic signals generated by the conveying the wheat grains in the pipe, the SENNHEISER (ew100 ENG G3 series) which includes a microphone (ME2 model), a receiver (EC 100 G3 model) and a portable transmitter (SK 100 G3), was used. This set has a frequency response of 25 to 18000 Hz, which is very suitable for fast dynamic responses. In order to record the acoustic signals of wheat grains in the pneumatic conveying, the microphone was mounted on the transmission pipe (Fig. 1). To remove the noise of the environment, the microphone was placed inside the foam and completely covered by the glass wool. Also, to reduce the sound produced by the cyclone separator, its outer part was completely covered by glass wool. Acoustic signals stored online through the oscilloscope section of the Matlab software.


**Fig 1 - Schematic of wheat grains conveying system and acoustic signals recording system**

- **Signal processing**

The received acoustic signals from wheat grains (at three mass flow rate levels of 1.5, 3 and 4.5 kg/min) were processed in time-frequency domain using wavelet transform. In wavelet transformation, the signal is passed through a series of upstream and downstream filters. Signal is divided in two parts; the section, which passes from a high-pass filter, contains high frequency data i.e. noise. It is called details. The second section, which passes from a low–pass filter, contains low frequency data and includes features of signals and is called approximations. In general, if x(t) is the main signal and using the wavelet is decomposed into n levels, the first signal can be achieved from the sum of approximation signals at the last level and sum of the detail functions at different levels and calculated from equation below (*Soman, 2010; Zanardelli et al., 2005*):

$$x(n) = a_n(n) + \sum_{n=1}^{N} d_n(n) \tag{1}$$

Decomposition operations can be continued until there is no significant data in approximations. So, the first signal can be rebuilt using details signals without losing any necessary data. Selection of function type is different for various problems in wavelet transformation. The Daubechi function (DB3) has been used at the most of studies. The efficiency of Daubechi function is acknowledged. Hence, the mentioned function is used in this research to decompose the acoustic signals. So, Daubechi function with nine decomposition levels was selected after try and error. Therefore, the signal can be written as Equation (2), ($d_1$- $d_9$ are details and $a_9$ is approximation):

$$x[n] = a_9 + d_9 + d_8 + d_7 + d_6 + d_5 + d_4 + d_3 + d_2 + d_1 \tag{2}$$

Where x[n] is the main signal and indices are related to the decomposition level of signal.

In order to detect signals pertaining to several different mass flow levels and finally to differentiate these levels, the characteristic vector of the sub-signals should be selected and according to the changes in these vectors, the mass flow levels can be differentiated. In this study, Sum, Mean, Variance, Root Mean Square (RMS), Skewness, Kurtosis and Moment were used to compare the output signals of different mass flow levels.

*SUM*

The sum is the total amplitude of acoustic signal data points that can indicate the intensity of the acoustic signal and is defined mathematically as below (*Lei et al., 2008*):

$$Sum = \sum_{n=1}^{N} x(n) \tag{3}$$

Where, $x(n)$ is the amplitude of data points.

*AVERAGE (MEAN)*

As much as the average value becomes closer to zero, symmetry of the signal of the system increases. Because the vibrational and acoustic signals are in wave forms, the signal value is usually zero. So, to use this factor, the absolute function is used. Its mathematical equation is as below (*Lei et al., 2008*):

$$Mean(abs) = \frac{\sum_{n=1}^{N} abs(x(n))}{N} \tag{4}$$

*VARIANCE (VAR)*

This factor usually indicates the dispersion of the signal. Whatever the magnitude of the variance, the signal is more uniform and more aggressive. In other words, the received sound is more turbulent and inconsistent (*Lei et al., 2008*).

$$Var(x(n)) = \frac{\sum_{n=1}^{N} \left(x(n) - mean(x(n))\right)^2}{N-1} \tag{5}$$

*ROOT MEAN SQUARE (RMS)*

One of the most commonly used value in acoustic signals analysis, is the Root Mean Squared (RMS). Because the most important property of an acoustic signal is the content of its energy. The energy is proportional to the signal amplitude, and a second-power average will better than the power of the acoustic signal. RMS is calculated as equation 6 *(Mohammed et al., 2013*):

$$RMS = \left[ \frac{\sum_{n=1}^{N} (x(n))^2}{N} \right]^{1/2} \tag{6}$$

In which $x(n)$ is the amplitude of data point and *N* is the number of signal data point.

*SKEWNESS*

This parameter shows the elongation of the signal to one side (*Khazaee et al., 2013*).

$$Skewness = \frac{\frac{1}{n}\sum_{n=1}^{N} \left(x(n) - mean(x(n))\right)^3}{\left(\frac{1}{n}\sum_{n=1}^{N}\left(x(n) - mean(x(n))\right)^2\right)^{3/2}} \tag{7}$$

*KURTOSIS*

Kurtosis indicates the magnitude and sharpness of the extremes of signals. In fact, the larger Kurtosis indicates that the pulses of the larger system have a bigger, sharper and wider sequence. Kurtosis is used to detect the defects of microstructures. The existence of fine flaws in a structure will increase the distortion of the signal and increase the amount of Kurtosis signal. The value of Kurtosis for random and digital signals x (n) with the number of N data, is calculated as equation 8 *(Mohammed et al., 2013*):

$$kurtosis = \frac{\frac{1}{N}\sum_{n=1}^{N} x(n)^4}{\left[\frac{1}{N}\sum_{n=1}^{N} x(n)^2\right]^2} \tag{8}$$

*MOMENTUM (MOMENT)*

This factor represents the normalized value of the signal relative to the mean, and is an appropriate factor for checking the signal's impact status ( *Khazaee et al., 2013*):

$$Moment(4) = \frac{\sum_{n=1}^{N}\left(x(n) - Mean(x(n))\right)^4}{N} \tag{9}$$

- **Statistical analysis**

The test was performed for each rate with 30 repetitions, and a total of 90 signals were obtained. Signal processing was performed using the MTLAB software. The Duncan method was used to compare the averages at 1% and 5% probability. SAS9.1 software was used for statistical analyzes.

## RESULTS

In Fig. 2, the signals related to three mass flow levels of 1.5 kg/min, 3 kg/min and 4.5 kg/min are shown.

A)

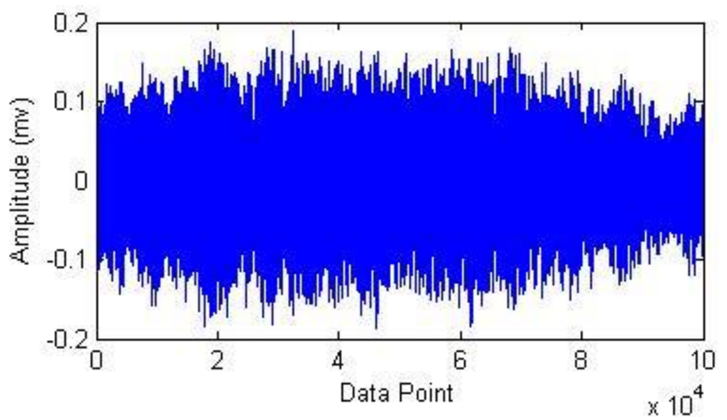


B)

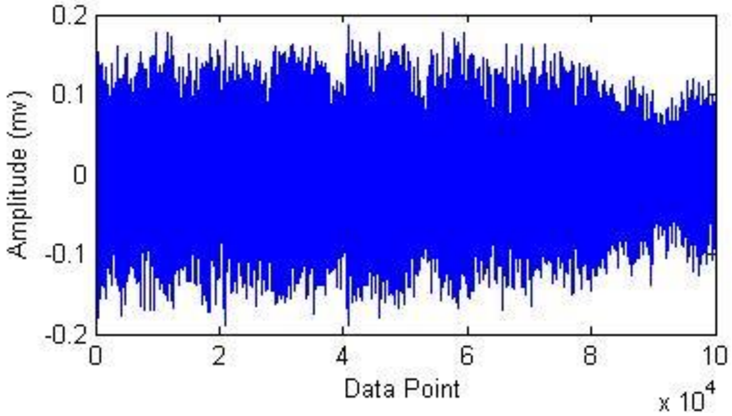


C)

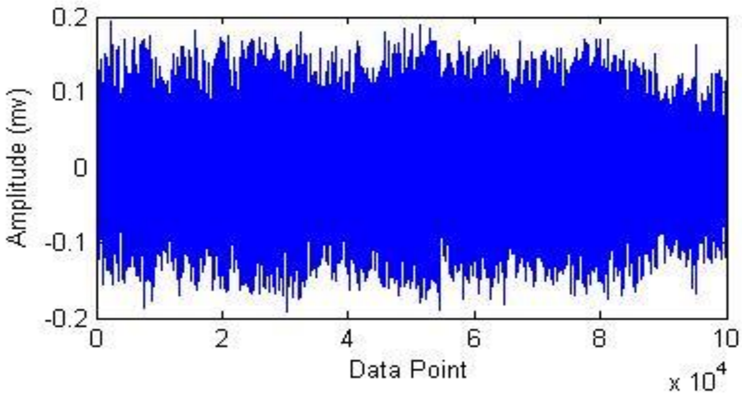


**Fig. 2 - Acoustic signals related to different mass flow levels**
**A)** ***1.5 kg/min*** **B)** ***3 kg/min*** **and C)** ***4.5 kg/min***

As shown in fig. 2, the signals related to the three different mass flow levels are similar and separation of mass flow levels is not possible. Therefore, the signals received from different mass flow levels were decomposed using the wavelet transform to the detail sub-signals of 1 to 9 ($d_1$ to $d_9$) and 9th approximate ($a_9$) to allow detection of mass flow levels from each other.

Fig.3 and fig. 4 show the decomposed signals for each mass flow levels.

A)

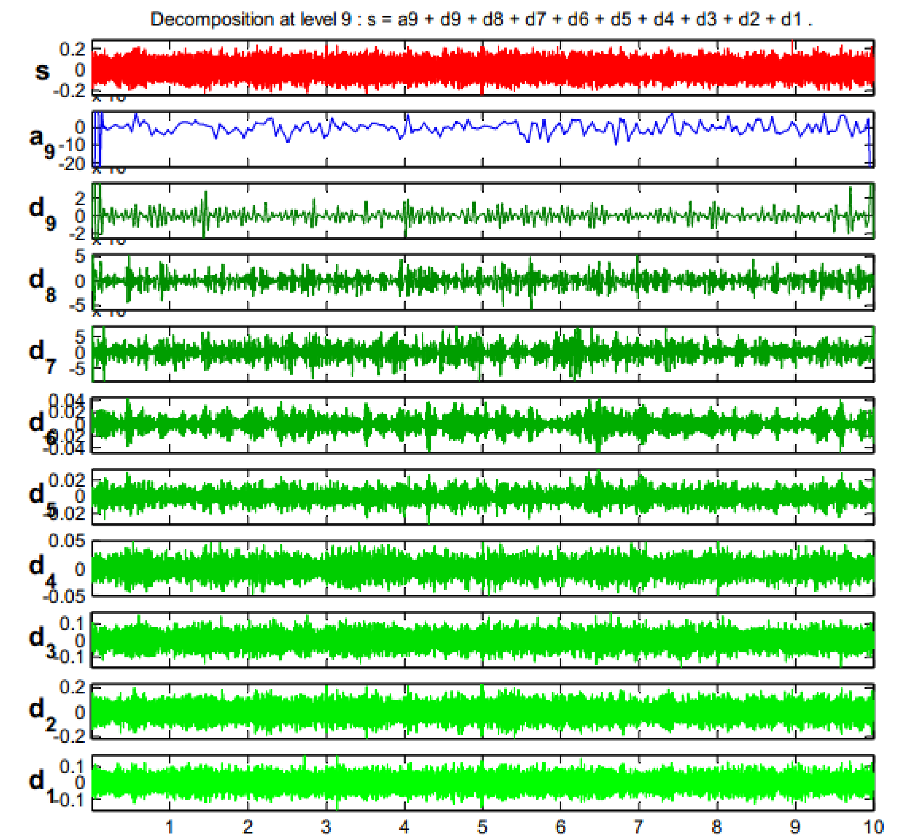


B)

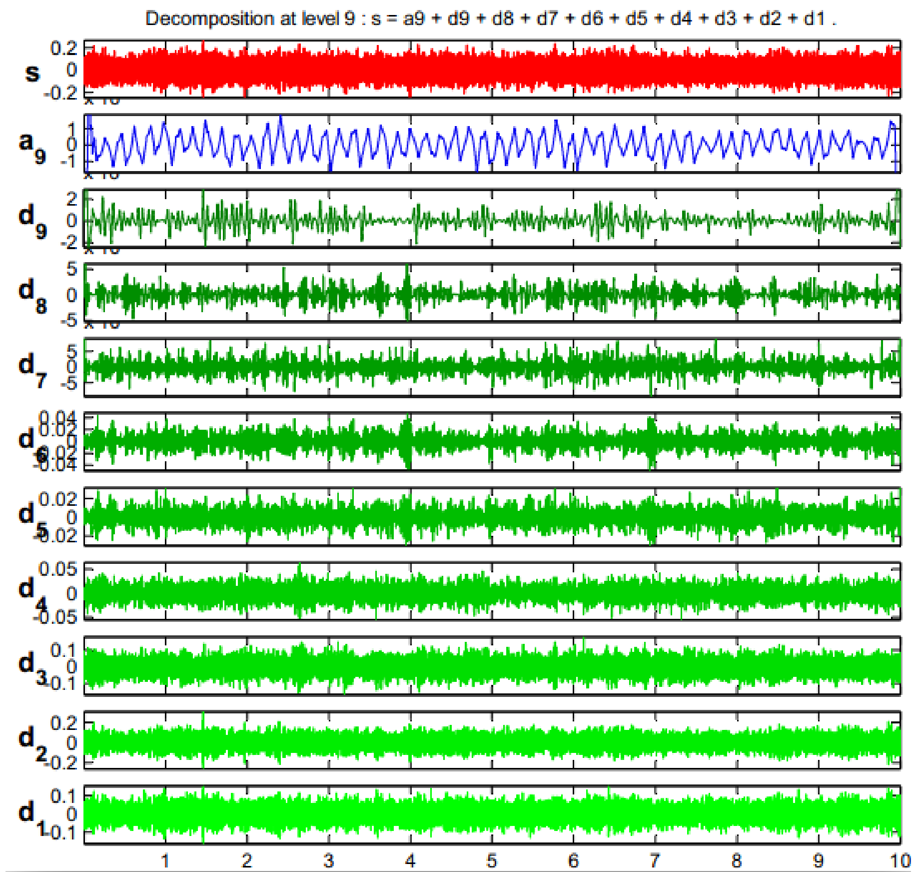


**Fig. 3- Decomposing the main signals to detail and approximate sub-signals, A) 1.5 kg/min and B) 3 kg/min**

C)

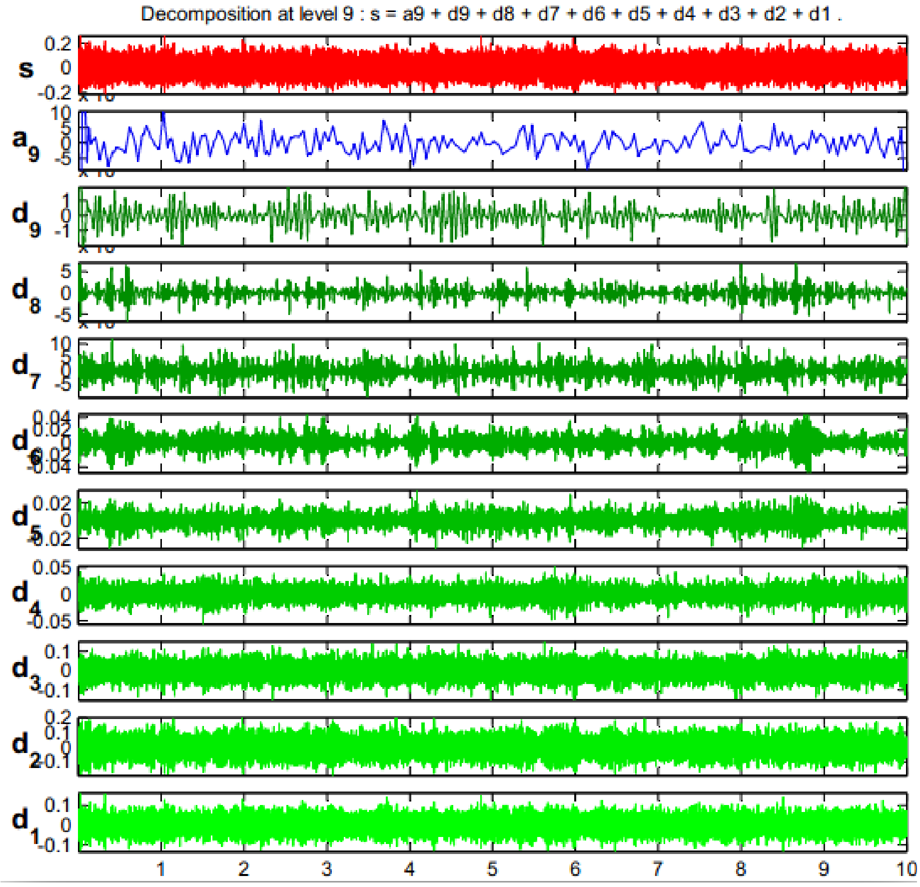


**Fig. 4- Decomposing the main signals to detail and approximate sub-signals**
**C) 4.5 kg/min**

In order to detect the difference in mass flow levels signals using sub-signals, seven characteristics of Sum, Mean, Variance (VAR), RMS, Skewness, Kurtosis and Moment were used. Comparison of these characteristics at the probability level of 1% and 5% for $d_1$ to $d_9$ and $a_9$ are presented in Tables 2 to 10, respectively.

**Table 2**

**Characteristics of the first detail ($d_1$) sub-signal**

| Mass flow rate [kg/min] | Signal properties | | | | | | |
|---|---|---|---|---|---|---|---|
| | **Sum** | **Mean** | **VAR** | **RMS** | **Skewness** | **Kurtosis** | **Moment** |
| 1.5 | 613$^{a}$ | 0.0076$^{a}$ | 9.97E-05$^{a}$ | 0.0100$^{a}$ | -0.0193$^{a'}$ | 3.51$^{a'}$ | 3.5E-08$^{a}$ |
| 3 | 684$^{b}$ | 0.0085$^{b}$ | 0.000123$^{b}$ | 0.0111$^{b}$ | -0.0185$^{a'}$ | 3.37$^{b'}$ | 5.1E-08$^{b}$ |
| 4.5 | 754$^{c}$ | 0.0094$^{c}$ | 0.000149$^{c}$ | 0.0122$^{c}$ | -0.0135$^{a'}$ | 3.29$^{c'}$ | 7.3E-08$^{c}$ |

*Different superscript indicates significant differences at the level of 1% (normal) and 5% (with Prim).*

**Table 3**

**Characteristics of the second detail ($d_2$) sub-signal**

| Mass flow rate [kg/min] | Signal properties | | | | | | |
|---|---|---|---|---|---|---|---|
| | **Sum** | **Mean** | **VAR** | **RMS** | **Skewness** | **Kurtosis** | **Moment** |
| 1.5 | 1292$^{a}$ | 0.0161$^{a}$ | 0.00044$^{a}$ | 0.0209$^{a}$ | -0.0140$^{a'}$ | 3.50$^{a'}$ | 6.75E-07$^{a}$ |
| 3 | 1383$^{b}$ | 0.0173$^{b}$ | 0.00050$^{b}$ | 0.0223$^{b}$ | -0.0091$^{a'}$ | 3.41$^{a'}$ | 8.5E-07$^{b}$ |
| 4.5 | 1494$^{c}$ | 0.0187$^{c}$ | 0.00057$^{c}$ | 0.0240$^{c}$ | -0.0115$^{a'}$ | 3.27$^{b'}$ | 1.1E-06$^{c}$ |

Table 4

**Characteristics of the third detail ($d_3$) sub-signal**

| Mass flow rate [kg/min] | Signal properties | | | | | | |
|---|---|---|---|---|---|---|---|
| | Sum | Mean | VAR | RMS | Skewness | Kurtosis | Moment |
| 1.5 | $2552^{a'}$ | $0.0319^{a'}$ | $0.00176^{a'}$ | $0.0420^{a'}$ | $-0.00053^{a'b'}$ | $4.13^{a'}$ | $1.29E-05^{a'}$ |
| 3 | $2537^{a'}$ | $0.0317^{a'}$ | $0.00175^{a'}$ | $0.0417^{a'}$ | $-0.00978^{a'}$ | $4.08^{a'}$ | $1.26E-05^{a'}$ |
| 4.5 | $2656^{a'}$ | $0.0332^{a'}$ | $0.00192^{a'}$ | $0.0438^{a'}$ | $0.00433^{b'}$ | $4.11^{a'}$ | $1.52E-05^{a'}$ |

Table 5

**Characteristics of the fourth detail ($d_4$) sub-signal**

| Mass flow rate [kg/min] | Signal properties | | | | | | |
|---|---|---|---|---|---|---|---|
| | Sum | Mean | VAR | RMS | Skewness | Kurtosis | Moment |
| 1.5 | $1213^{a'}$ | $0.0151^{a'}$ | $0.000434^{a'}$ | $0.0208^{a'}$ | $0.0056^{a'}$ | $5.059^{a'}$ | $9.52E-07^{a'}$ |
| 3 | $1189^{a'}$ | $0.0148^{a'}$ | $0.000422^{a'}$ | $0.0205^{a'}$ | $0.0037^{a'}$ | $5.108^{a'}$ | $9.17E-07^{a'}$ |
| 4.5 | $1283^{a'}$ | $0.0160^{a'}$ | $0.000488^{a'}$ | $0.0221^{a'}$ | $-0.0076^{a'}$ | $5.143^{a'}$ | $1.23E-06^{a'}$ |

Table 6

**Characteristics of the fifth detail ($d_5$) sub-signal**

| Mass flow rate [kg/min] | Signal properties | | | | | | |
|---|---|---|---|---|---|---|---|
| | Sum | Mean | VAR | RMS | Skewness | Kurtosis | Moment |
| 1.5 | $495^{a}$ | $0.0062^{a}$ | $7.43E-05^{a}$ | $0.0086^{a}$ | $0.0035^{a'}$ | $5.827^{a'}$ | $3.20E-08^{a'}$ |
| 3 | $576^{b}$ | $0.0072^{b}$ | $9.8E-05^{b}$ | $0.0099^{b}$ | $0.0492^{a'}$ | $5.508^{a'b'}$ | $5.31E-08^{b'}$ |
| 4.5 | $686^{c}$ | $0.0086^{c}$ | $0.00013^{c}$ | $0.0116^{c}$ | $0.0084^{a'}$ | $5.069^{b'}$ | $9.25E-08^{c'}$ |

Table 7

**Characteristics of the sixth detail ($d_6$) sub-signal**

| Mass flow rate [kg/min] | Signal properties | | | | | | |
|---|---|---|---|---|---|---|---|
| | Sum | Mean | VAR | RMS | Skewness | Kurtosis | Moment |
| 1.5 | $405^{a}$ | $0.0051^{a}$ | $4.83E-05^{a}$ | $0.0069^{a}$ | $-0.0091^{a'}$ | $5.28^{a'}$ | $1.24E-08^{a'}$ |
| 3 | $487^{b}$ | $0.0061^{b}$ | $6.83E-05^{b}$ | $0.0082^{b}$ | $0.0059^{a'}$ | $5.19^{a'}$ | $2.41E-08^{b'}$ |
| 4.5 | $579^{c}$ | $0.0072^{c}$ | $9.56E-05^{c}$ | $0.0098^{c}$ | $-0.0193^{a'}$ | $4.80^{a'}$ | $4.40E-08^{c'}$ |

Table 8

**Characteristics of the seventh detail ($d_7$) sub-signal**

| Mass flow rate [kg/min] | Signal properties | | | | | | |
|---|---|---|---|---|---|---|---|
| | Sum | Mean | VAR | RMS | Skewness | Kurtosis | Moment |
| 1.5 | $375^{a'}$ | $0.0047^{a'}$ | $4.03E-05^{a'}$ | $0.0063^{a'}$ | $0.116^{a'}$ | $5.28^{a'}$ | $8.54E-09^{a'}$ |
| 3 | $430^{b'}$ | $0.0054^{b'}$ | $5.24E-05^{b'}$ | $0.0072^{b'}$ | $0.068^{a'}$ | $4.98^{a'b'}$ | $1.39E-08^{a'b'}$ |
| 4.5 | $483^{c'}$ | $0.0060^{c'}$ | $6.55E-05^{c'}$ | $0.0081^{c'}$ | $-0.041^{b'}$ | $4.62^{b'}$ | $2.00E-08^{b'}$ |

Table 9

**Characteristics of the eighth detail ($d_8$) sub-signal**

| Mass flow rate [kg/min] | Signal properties | | | | | | |
|---|---|---|---|---|---|---|---|
| | Sum | Mean | VAR | RMS | Skewness | Kurtosis | Moment |
| 1.5 | $330^{a'}$ | $0.00412^{a'}$ | $2.99E-05^{a'}$ | $0.0054^{a'}$ | $-0.0262^{a'}$ | $4.29^{a'}$ | $3.92E-09^{a'}$ |
| 3 | $361^{a'}$ | $0.00451^{a'}$ | $3.72E-05^{a'}$ | $0.0061^{b'}$ | $-0.0054^{a'}$ | $4.56^{a'}$ | $6.30E-09^{a'b'}$ |
| 4.5 | $399^{b'}$ | $0.00499^{b'}$ | $4.48E-05^{b'}$ | $0.0067^{b'}$ | $-0.0341^{a'}$ | $4.51^{a'}$ | $9.24E-09^{b'}$ |

**Table 10**

**Characteristics of the ninth detail ($d_9$) sub-signal**

| Mass flow rate [kg/min] | Signal properties | | | | | | |
|---|---|---|---|---|---|---|---|
| | Sum | Mean | VAR | RMS | Skewness | Kurtosis | Moment |
| 1.5 | 169$^{a'}$ | 0.0021$^{a'}$ | 8.30E-06$^{a'}$ | 0.00287$^{a'}$ | 0.174$^{a'}$ | 4.59$^{a'}$ | 3.4E-10$^{a'}$ |
| 3 | 183$^{a'}$ | 0.0023$^{a'}$ | 9.48E-06$^{a'}$ | 0.00308$^{a'}$ | 0.037$^{a'}$ | 4.83$^{a'}$ | 4.4E-10$^{a'}$ |
| 4.5 | 220$^{b'}$ | 0.0027$^{b'}$ | 1.35E-05$^{b'}$ | 0.00368$^{b'}$ | 0.014$^{a'}$ | 4.79$^{a'}$ | 8.8E-10$^{b'}$ |

**Table 11**

**Characteristics of the ninth detail ($a_9$) signal**

| Mass flow rate [kg/min] | Signal properties | | | | | | |
|---|---|---|---|---|---|---|---|
| | Sum | Mean | VAR | RMS | Skewness | Kurtosis | Moment |
| 1.5 | 119$^{a'}$ | 0.00149$^{a'}$ | 3.87E-06$^{a'}$ | 0.00198$^{a'}$ | 0.1307$^{a'}$ | 4.29$^{a'}$ | 6.57E-11$^{a'}$ |
| 3 | 144$^{b'}$ | 0.00179$^{b'}$ | 5.52E-06$^{b'}$ | 0.00234$^{b'}$ | -0.0845$^{a'}$ | 3.89$^{a'}$ | 1.18E-10$^{a'}$ |
| 4.5 | 154$^{b'}$ | 0.00192$^{b'}$ | 6.53E-06$^{b'}$ | 0.00256$^{b'}$ | 0.019$^{a'}$ | 4.29$^{a'}$ | 1.83E-10$^{b'}$ |

In Table 2, the first detail ($d_1$) sub-signal at the probability of 1% and using the Sum, Mean, VAR, RMS and Moment can detect various mass flow levels as well as the Kurtosis at the probability of 5%. According to the Table 3, the second detail ($d_2$) sub-signal at 1% probability has the same behavior as the first detail sub-signal ($d_1$) and with the four characteristics of Sum, Mean, VAR, RMS and Moment can differentiate the mass flow levels. According to the results of Tables 4 and 5, the third and fourth details ($d_3$ & $d_4$) sub-signals are unable to detect different mass levels with any of the characteristics. As can be seen in Table 6, in the fifth detail ($d_5$) sub-signals, the difference between the values of Sum, Mean, VAR, RMS at the probability level of 1% and Moment at a probability level of 5% and at different mass flow levels, is significant and these sub-signals can differentiate mass flow levels. The results of the sixth detail ($d_6$) in Table 7 show that the conditions of this sub-signal are exactly the same as the fifth detail sub-signals and will have the differentiation capability by using the four properties of Sum, Mean, VAR, RMS at the probability level of 1% and using the moment property at probability level 5 %. As shown in Table 8, the seventh detail ($d_7$) sub-signal has the ability to detect mass flow levels in each of the four properties of Sum, Mean, VAR, RMS at a 5% probability level. According to Tables 9 and 10, the eighth and ninth details ($d_8$ & $d_9$) sub-signal are not capable of detecting and differentiating the different levels of mass flow levels by using any of the properties. Also, according to Table 11, the ninth approximate ($a_9$) will not be able to detect different levels of mass flow levels from each other. Table 12 shows the prioritization of the first to ninth ($d_1$ to $d_9$) sub-signals and the ninth approximate ($a_9$) according to the probability levels of 1% and 5%.

**Table 12**

**Prioritization of mass flow detection by sub-signals and characteristics**

| Sub-signals | Probability Level | Characteristics |
|---|---|---|
| $d_1$ | 1% | Sum, Mean, VAR, RMS and Moment |
| | 5% | Kurtosis |
| $d_2$ | 1% | Sum, Mean, VAR, RMS and Moment |
| $d_5$ & $d_6$ | 1% | Sum, Mean, VAR, RMS |
| | 5% | Moment |
| $d_7$ | 5% | Sum, Mean, VAR, RMS |
| $d_3$ & $d_4$ & $d_8$ & $d_9$ & $a_9$ | Non-significant | - |

According to Table 12, the first ($d_1$), second ($d_2$), fifth ($d_5$), sixth ($d_6$) and seventh ($d_7$) detail sub signals, can be used to determine the different mass flow levels according to priority. On the other hand, the third ($d_3$), fourth ($d_4$), seventh ($d_7$), eighth ($d_8$), and the ninth ($a_9$) approximate sub signals, will not be able to detect. The cause of the sub-signals of the separable details in the characteristics of the effective signal is that the frequency of disturbing sound signals, such as the centrifugal fan and the cyclone, is not present in these details, resulting in lower noise disturbance and the ability to separate them in the details.

## CONCLUSIONS

In this study, the acoustic signal analysis technique potential was evaluated to determine the mass flow rate of wheat grains in pneumatic conveying. The acoustic signals of three levels of mass flow rate includes: 1.5 kg/min, 3 kg/min and 4.5 kg/min were measured by a microphone that located in elbow section of pipe. To more detailed research, signals were decomposed using wavelet transform into 9 sub-signals and 7 characteristics of sub-signals including: Sum, Mean, VAR, RMS, Kurtosis, Skewness and Moment were compared. The main results of the present work can be summarized as following:

(1) Among sub-signals, maximum effect of mass flow rate variation was related to $d_1$, $d_2$, $d_3$ and $d_4$ sub-signals, respectively and these sub-signals have more potential to recognize the various mass flow rate levels.

(2) Among characteristics, the effect of mass flow rate variation on characteristics (Sum, Mean, VAR and RMS) in all 4 sub-signals ($d_1$, $d_2$, $d_3$ and $d_4$) was significant at probability levels of 1%. So, these characteristics, in mentioned sub-signals have more potential to recognize the various mass flow rate levels. Also, the effect of mass flow rate variation on the characteristic of Moment in $d_1$ and $d_2$ sub-signals was significant at probability levels of 1% and in $d_5$ and $d_6$ sub-signals was significant at probability levels of 5%.

(3) All of these characteristics were increased by increasing mass flow rate levels, which is due to the amplification of the acoustic signal frequencies and increase in sound received by the microphone.

Over the years, various sensing techniques have been developed and proposed to measure the particle mass flow rate. Among them, the most promising methods are electrostatic, microwave and tomographic methods. These methods are limited in their industrial application, because they are either sensitive to the change of environment, expensive and time-consuming. But, the acoustic signals analysis is attractive because of its advantages such as the relevance of the optimum frequency with particle size, the simplicity of the method, the robustness against difficult conditions, easy installation, online display, equipment costs and low maintenance. Moreover, the results of this study were showed the performance of this technique. Thus, the acoustic signal analysis technique holds a great potential to recognize the particle mass flow rate in pneumatic conveying and other particulate processes.

## REFRENCES


[1] Dhoriyani M.L., Mukesh L., Jonnalagad d., Kranthi K., Kandikatla R.K., Rao K., (2006), Silo music: sound emission during the flow of granular materials through tubes. *Powder Technology,* Vol.167, Issue 2, pp. 55-71, India;

[2] Fuchs A., Zangl H., (2008), Measuring flow parameters of particulate and powdery solids in industrial transportation processes. *International journal on smart sensing and systems*, Vol.1, Issue 2, pp. 388-402, Austria;

[3] He L., Zhou Y., Huang Z., Wang J., Lungu M., Yang Y., (2014), Acoustic analysis of particle–wall interaction and detection of particle mass flow rate in vertical pneumatic conveying, *Industrial & Engineering Chemistry Research*, Vol.53, Issue 23, pp. 9938-9948, China;

[4] Khazaee M., Ahmadi H., Omid M., Banakar A., Moosavian A., (2013), Feature-level fusion based on wavelet transform and artificial neural network for fault diagnosis of planetary gearbox using acoustic and vibration signals, *Insight-NonDestructive Testing and Condition Monitoring*, Vol.55, Issue 6, pp. 323-330, Iran;

[5] Klinzing D.C., Madoff L.C., Puopolo K.M., (2009), Genomic analysis identifies a transcription-factor binding motif regulating expression of the alpha C protein in Group B Streptococcus. *Microb Pathog*, Vol.46, Issue 6, pp. 315-20, American;

[6] Lei U., He Z., Zi Y., (2008), A new approach to intelligent fault diagnosis of rotating machinery, *Expert Systems with Applications*, Vol.35, pp. 1593-1600, China;

[7] Mills D., (2013), *Pneumatic conveying design guide*, chapter 1, Butterworth-Heinemann, ISBN 0 7506 5471 6, Chennai/India;

[8] Mohammed O.D., Rantatalo M., Aidanpää J.O., Kumar U., (2013), Vibration signal analysis for gear fault diagnosis with various crack progression scenarios, *Mechanical Systems and Signal Processing*, vol.41, pp. 176-195, Sweden;

[9] Soman K.P., (2010), *Insight into wavelets:* Front Cover. K. P. Soman. PHI Learning Pvt. Ltd., 2010 - Wavelets (Mathematics), 447 p.;

[10] Sun D., Yan Y., Carter R.M., Gao L., Lu G., Riley G., Wood M., (2014), On-line nonintrusive detection of wood pellets in pneumatic conveying pipelines using vibration and acoustic sensors, *IEEE Transactions on Instrumentation and Measurement,* Vol.63, Issue 5, pp. 993-1001, UK;

[11] Tallon S.J., Davies C.E., (2000), The effect of pipeline location on acoustic measurement of gas–solid pipeline flow. *Flow Measurement and Instrumentation*, Vol.11, Issue 3, pp. 165-169, New Zealand;

[12] Van Y., Byrne B., Coulthard J., (1993), Radiation attenuation of pulverised fuel in pneumatic conveying systems, *Transactions of the Institute of Measurement and Control,* Vol.15, Issue 3, pp. 98-103, California;

[13] Yan Y., (1996), Mass flow measurement of bulk solids in pneumatic pipelines, *Measurement Science and Technology,* Vol.7, Issue 12, pp. 1687-1706, UK;

[14] Zanardelli W.G., Strangas E., Khalil H.K., Miller J.M., (2005), Wavelet-based methods for the prognosis of mechanical and electrical failures in electric motors. *Mechanical Systems and Processing*, Signal, Vol.19, Issue 2, pp. 411-426, USA;

[15] Zheng Y., Liu Q., (2011), Review of techniques for the mass flow rate measurement of pneumatically conveyed solids. *Measurement,* Vol.44, Issue 4, pp. 589-604, PR China.